Eur. Phys. J. D **18**, 295–300 (2002)
DOI: 10.1140/epjd/e20020033

THE EUROPEAN PHYSICAL JOURNAL D
EDP Sciences

Individual and center-of-mass resonances in the motional spectrum of an electron cloud in a Penning trap

P. Paasche, T. Valenzuela, D. Biswas[a], C. Angelescu, and G. Werth[b]

Johannes Gutenberg University, Institut fuer Physik, 55099 Mainz, Germany

Received 11 July 2001 and Received in final form 12 November 2001

Abstract. We have examined experimentally the motional spectrum of an electron cloud confined in a Penning trap. When the axial oscillation is excited by a radio frequency field the resonance exhibits a double structure. Both components depend differently on the number of trapped electrons and have different shape and width. We conclude that one of them corresponds to the excitation of the individual electrons while the other is the center-of-mass mode of the cloud. The threshold behaviour of the center-of-mass resonance suggests that it is a parametric instability of a Mathieu type equation of motion.

PACS. 52.27.Jt Nonneutral plasmas – 82.80.Qx Ion cyclotron resonance mass spectrometry

1 Introduction

A cloud of charged particles confined by electro-magnetic fields can serve for high precision atomic and nuclear spectroscopy [1,2], for collision studies [3], mass spectrometry [4] or quantum optics experiments [5]. It can also be considered as excellent microlaboratory for the investigation of nonlinear dynamics [6]. It is of particular interest to study the properties of a cloud of trapped charged particles when it is considered as a charged single-component plasma [7]. Recent investigations have concentrated on the investigation of laser cooled ionic plasmas which form a spheroid of uniform density [8]. The strong coupling between the ions at low temperatures leads to crystalline orders which can be imaged using suitable detection techniques [9]. The electrostatic modes of such a plasma can be calculated analytically [10,11]. A cold fluid theory [12] predicts the frequencies of plasma modes which have been observed experimentally on a cloud of laser cooled Be^+ ions [8,13].

Work on trapped electron plasmas deals with higher temperatures and low densities as no laser cooling can be employed. Tinkle *et al.* [14] measured the dependence of plasma mode frequencies on aspect ratio and temperature. Weimer *et al.* [15] found a way to increase the plasma density of the electrons by magnetron sideband cooling technique [16]. Using a theoretical model [12] they could determine density, aspect ratio, and size of the electron plasma.

In the work reported here we have performed measurements on the axial mode of trapped electrons in a Penning trap at high temperatures in order to confirm and investigate in more detail earlier reports on oscillations of an "annealed" electron cloud [17]. They were triggered by similar observations on a hot ion cloud in a radio-frequency trap where "collective" and "non-collective" axial oscillations could be distinguished [18].

2 Experiment

Our experiments are carried out in a Penning trap [16,19] with hyperbolic shaped electrode surfaces. We define the axis of symmetry as z-axis. The potential inside the trap in the absence of particles is the well-known quadrupole potential

$$\phi = \frac{V}{r_0^2}\left(r^2 - 2z^2\right) \tag{1}$$

r_0 is the radius of the ring electrode. The quadratic dependence of the potential on the distance from the trap center ensures a linear dependence of the forces acted upon the charges particles by the electric field. A negative dc voltage at the endcap electrodes leads to axial confinement of electrons. Radial confinement is achieved by the superposition of a magnetic field in axial direction.

For a single electron with charge e inside the trap the equation of motion can easily be written down:

$$\begin{aligned} m\ddot{x} + e\dot{y}B + \frac{eV}{{r_0}^2}x &= 0 \\ m\ddot{y} - e\dot{x}B + \frac{eV}{{r_0}^2}y &= 0 \\ m\ddot{z} + \frac{eV}{{r_0}^2}z &= 0. \end{aligned} \tag{2}$$

[a] *Present address*: Dept. of Physics, Rampurhat College, Rampurhat, Birbhum, West Bengal, India.
[b] e-mail: werth@mail.uni-mainz.de
or e-mail: werth@dipmza.physik.uni-mainz.de

The solution of this set of equations are three harmonic oscillations with frequencies

$$\omega_{\rm c}' = \frac{\omega_{\rm c}}{2} + \sqrt{\left(\frac{\omega_{\rm c}}{2}\right)^2 - \frac{{\omega_z}^2}{2}}$$
$$\omega_{\rm m} = \frac{\omega_{\rm c}}{2} - \sqrt{\left(\frac{\omega_{\rm c}}{2}\right)^2 - \frac{{\omega_z}^2}{2}} \qquad (3)$$
$$\omega_z = \sqrt{\frac{eV}{2m{r_0}^2}}.$$

$\omega_{\rm c} = (e/m)B$ is the free electrons cyclotron frequency. $\omega_{\rm c}'$ is called the perturbed cyclotron frequency and $\omega_{\rm m}$ the magnetron frequency. When we confine not a single particle but many electrons the interacting Coulomb potential between the electrons has to be added to the confining quadrupole potential. Then the forces are no longer linear and the corresponding equations of motions can not be solved analytically any more. When we average over the individual electrons oscillation we can write the total potential in a series expansion in spherical harmonics $P(\cos\theta)$:

$$\Phi = \sum_{n=0}^{\infty} c_n \left(\frac{r}{r_0}\right)^n P_n(\cos\theta). \qquad (4)$$

The coefficients c_n denote the strength of the perturbing potentials. For $n = 2$ we have the unperturbed quadrupole potential.

The existence of higher order contributions to the potential has a number of consequences for the behaviour of the trapped particles:

(a) different degrees of freedom can not be separated any more as in equation (2) but mixed terms in all coordinates appear in the equations of motion leading to coupling between the radial and axial modes of oscillation. As a consequence we have not only the frequencies $\omega_{\rm c}'$, $\omega_{\rm m}$ and ω_z appearing in the motional spectrum but also linear combinations of them;
(b) the motion can not be described as harmonic oscillations but contains anharmonicities. Excitation of the motional resonances by an external radio-frequency field yields asymmetric line shapes, depending on the size of the coefficients c_n;
(c) coupling between the coordinates at higher order perturbations leads to energy transfer between the different degrees of freedom, a process which can contribute to electron loss from the trap.

In this paper we investigate experimentally the motional spectrum of electrons with a view to examining the predictions in (a) and (b). The observation and discussion of instabilities in the electrons motion will be described in detail in a following paper.

Our trap (Fig. 1) has a ring radius of $r_0 = 2$ cm. It was used previously in laser spectroscopic experiments and therefore required holes in the ring electrode and slits in the lower endcap. The magnetic field in the z-direction, produced by two coils of 60 cm diameter in approximate Helmholtz configuration, can be varied between 0 and 10 mT. Electrons are injected into the trap from a hot tungsten wire just above the upper endcap electrode by a positive electric pulse of 100 V amplitude and typically 10 ms length, applied to the filament. While the endcap electrodes are held at dc ground potential, a constant positive storage voltage is applied to the ring electrode for a preset time. This time could be varied between 10 ms to virtually infinitely. This is followed by a ramp. Figure 2 shows the timing of the voltages.

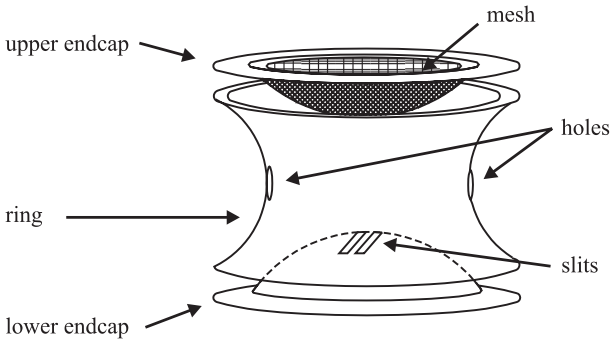

Fig. 1. Penning trap electrodes.

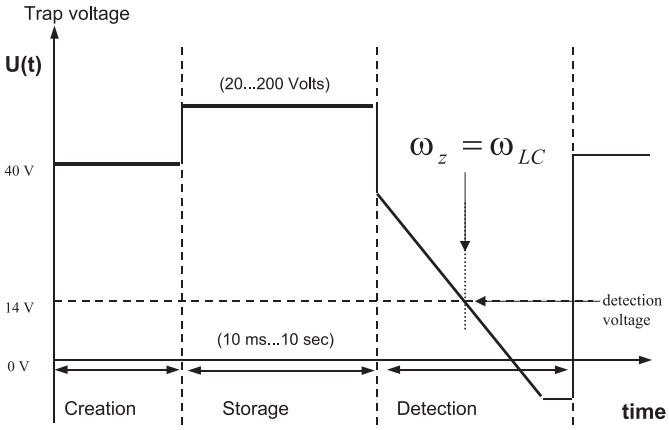

Fig. 2. Sequence of trapping voltages. When the electrons axial frequency coincides with the resonance frequency of a tank circuit, a detection signal is observed. When the ramp voltage changes sign the trap is emptied.

For detection of trapped electrons we apply a tank circuit consisting of an inductance and a capacitance in parallel to an endcap electrode. It is weakly excited at its resonance frequency $\omega_{\rm LC}$ (20 MHz). When the trapping voltage V is ramped down to a negative value the electrons axial frequency ω_z changes according to equation (3). For a particular value of the ramped trapping voltage it becomes coincident with $\omega_{\rm LC}$, leading to an energy transfer from the circuit to the electrons. The corresponding damping of the circuit is detected as a drop in the measured voltage across the endcaps. After rectification, we obtain a signal whose amplitude is proportional to the number of trapped trapped electrons. Figure 3 shows an example of a detection signal. It is digitized and further handled by a personal computer. The ramp voltage is lowered to a negative value to assure that all electrons leave the trap after

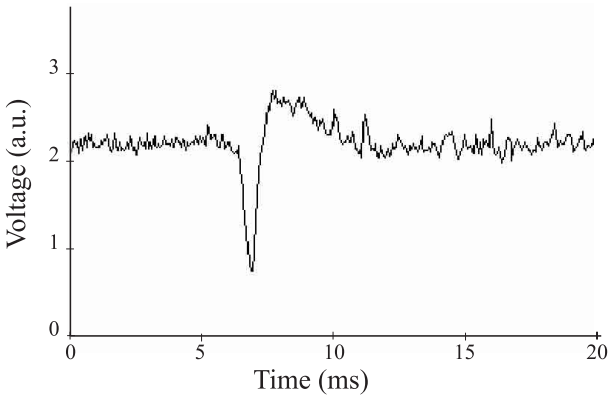

Fig. 3. Measured signal example.

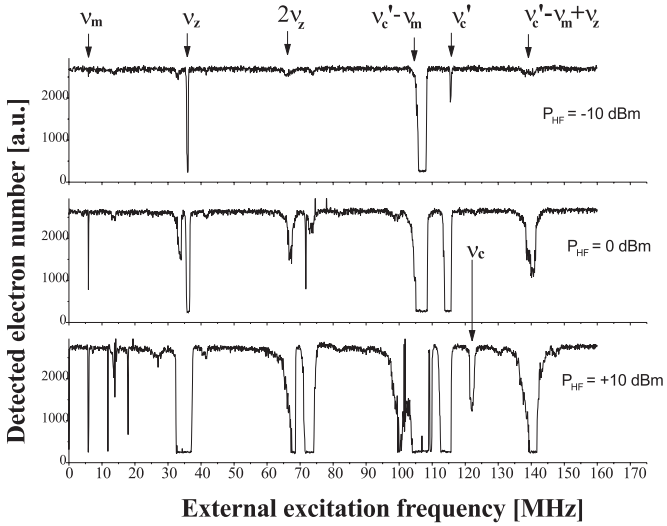

Fig. 4. Motional spectra for different rf-field amplitudes.

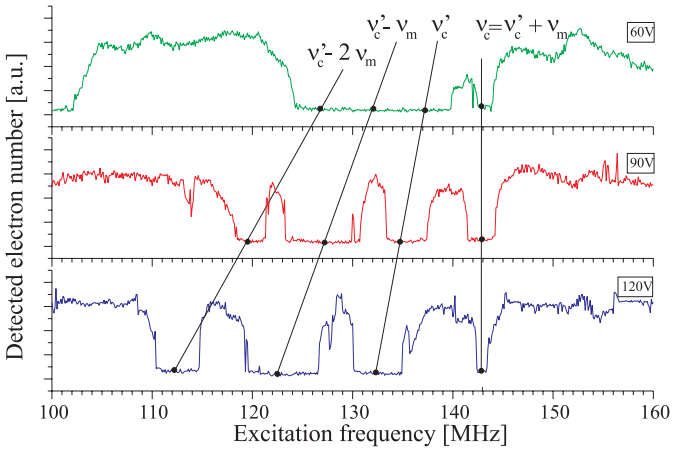

Fig. 5. Measured frequencies at different trap voltages.

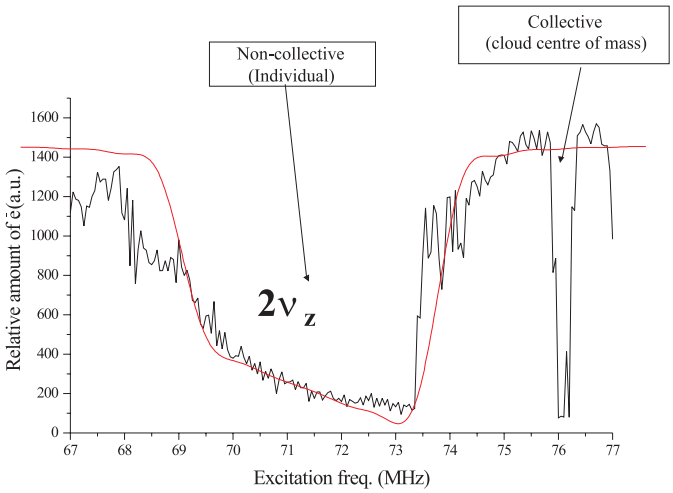

Fig. 6. Resonance at $2\omega_z$, showing two components. The asymmetric low frequency component has been modeled by numerical solution of the equation of motion assuming an octupole contribution to the trapping potential of strength $c_4 = 10^{-3}$ (dashed line).

being detected. Then a new cycle starts with a completely empty trap.

3 Motional resonances

The motional resonances are excited by sweeping the frequency of an externally applied rf-field. We used different ways to apply this field to the trap: (1) adding it to the dc potential, which results in a quadrupolar field geometry, (2) applying it between the two endcaps giving a dipole excitation, or (3) using an external antenna. The amplitude of the different motional resonances varied somewhat in different excitation modes but it had no influence of the particular observations of the axial resonances which are discussed below. Resonant excitation was detected as minima in the number of trapped electrons, as some of them absorb enough energy to leave the trap. Figure 4 shows such spectra taken at different amplitudes of the rf-field. A number of resonances are visible which appear, as expected, not only at the fundamental frequencies ω_c', ω_m and ω_z (Eq. (3)) but also at linear combinations of these frequencies.

The identification of the different resonances is by their different dependence on the trapping voltage, when the magnetic field is constant. Thus the magnetron frequency ω_m varies as V, whereas ω_z varies as $V^{1/2}$. ω_c' shows a small linear dependence on V. However the sideband $\omega_c' + \omega_m = \omega_c$, the free electron cyclotron frequency, should show no dependence on V. Figure 5 illustrates this fact.

4 Collective axial oscillation

We have examined the axial oscillation at $2\omega_z$ under higher resolution. This reveals the structure of a broad asymmetric minimum in the electron number, accompanied by a sharp resonance on the high frequency side (Fig. 6). The asymmetry of the low-frequency component arises from non-linearities in the trapping potential. We have approximately modeled the line shape by assuming an octupole contribution of strength $c_4 = 10^{-3}$ to the

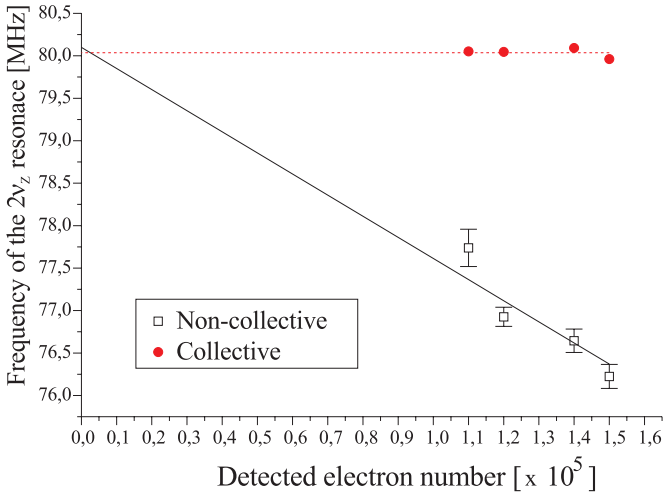

Fig. 7. Space charge effect in the non-collective and collective oscillations. The given error bars are 10% of the resonance full width. For the collective resonances they are of the order of the symbol size.

quadrupole potential ($c_2 = 1$) and numerically solving the equation of motion. The dashed line in Figure 6 is not a fit to the experimental data but a mere demonstration that in principle the shape of the resonance can be understood. More realistically one would have to take additional higher order contributions into account.

Both resonances show different dependencies on the number of trapped electrons: the broad, low frequency resonance gets shifted to lower frequencies, as the number of electrons increases. The number is estimated from the size of the shift when we use a simple model for the space charge potential [20]: when we assume for the electron cloud a uniformly charged sphere of density n, the shifted axial frequency can be written as

$$\omega_z' = \omega_z(1 - \alpha/3)^{1/2} \tag{5}$$

where

$$\alpha = \omega_\mathrm{p}^2/\omega_z^2 \tag{6}$$

with the plasma frequency

$$\omega_\mathrm{p}{}^2 = \frac{q^2 n}{\varepsilon_0 m}\,. \tag{7}$$

For small α the expected shift depends linear on the electron number as experimentally observed (Fig. 7). In contrast, the position of the sharp resonance remains invariant. The positions of both resonances coincide at the same frequency as the relative number of electrons goes to 0. A shift of the axial resonance might also appear by image charges induced in the trap electrodes. If in a simple model [21] the trap is replaced by a conducting spherical shell of radius a the image charge creates an electric field

$$\mathbf{E}_\mathrm{image} = \frac{nqa\mathbf{r}}{(a^2 - r^2)^2}\,. \tag{8}$$

This field is superimposed to the traps field and consequently shifts the electron oscillation frequencies. For the axial frequency this shift amounts for small n to

$$\Delta\omega_z = \frac{-nq^2}{2ma^3}\,. \tag{9}$$

Since our trap size is fairly large the calculated shift is by about 2 orders of magnitude smaller than the space charge shift and can be neglected. We conclude that the broad resonance is the incoherent oscillation of the different electrons in the cloud since the individual electrons are subject to the space charge potential of their neighbors while the sharp resonance represents the collective oscillation (center-of-mass) of the whole electron cloud. The observation of collective resonances in a trapped electron cloud has been reported earlier by Wineland and Dehmelt [17]. In a Paul radio-frequency trap confining atomic and molecular electrons they have also been observed and investigated in detail by Alheit *et al.* [18].

In order to understand the appearance of the collective resonance in the axial motion we consider the motion of the center of mass of the electron cloud in the Penning trap in the presence of an additional rf-field of quadrupolar geometry and include some damping mechanism, characterized by a damping constant γ

$$M\ddot{Z} + \gamma\dot{Z} + M{\omega_z}^2 Z = F_0 Z\cos\omega t. \tag{10}$$

Here M is the total mass of the electron cloud and F_0 the amplitude of the rf-field of frequency ω. Neglecting the damping for a moment this equation can be rewritten as

$$\ddot{Z} + {\omega_z}^2\left[1 - \frac{q}{{\omega_z}^2}\cos\omega t\right]Z = 0 \tag{11}$$

$$q = \frac{F_0}{M}{\omega_z}^2. \tag{12}$$

We substitute $\omega t = 2\tau$ and obtain

$$\ddot{Z} + \left(\frac{2\omega_z}{\omega}\right)^2\left[1 - \frac{4q}{{\omega_z}^2}\cos(2\tau)\right]Z = 0. \tag{13}$$

This is a Mathieu differential equation of the form

$$\ddot{Z} + [\hat{a} - 2\hat{q}\cos(2\tau)]Z = 0 \tag{14}$$

$$\hat{a} = \frac{4{\omega_z}^2}{\omega^2} \tag{15}$$

$$\hat{q} = \frac{8{\omega_z}^2}{\omega^2}\frac{F_0}{M}\,. \tag{16}$$

The solutions are known to become unstable for $\hat{a} = n^2$:n integer. For $n = 1$ it follows the observed center-of-mass resonance at $\omega = 2\omega_z$. The resonance appears, however, only when the amplitude of the exciting rf-field exceeds a critical value (Fig. 8). As pointed out in [18] the existence of a critical voltage requires a finite damping constant γ. From the electron number dependence of the critical voltage it was concluded in [18] that collisions of the electron cloud with molecules of the rest gas are responsible for

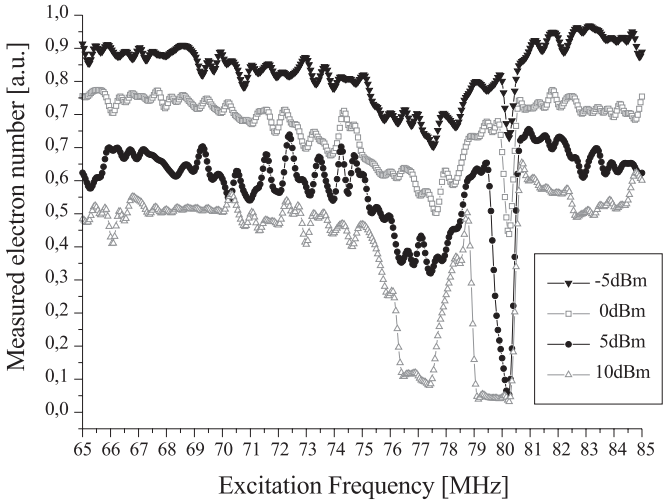

Fig. 8. The $2\omega_z$ resonance as a function of the rf-field amplitude.

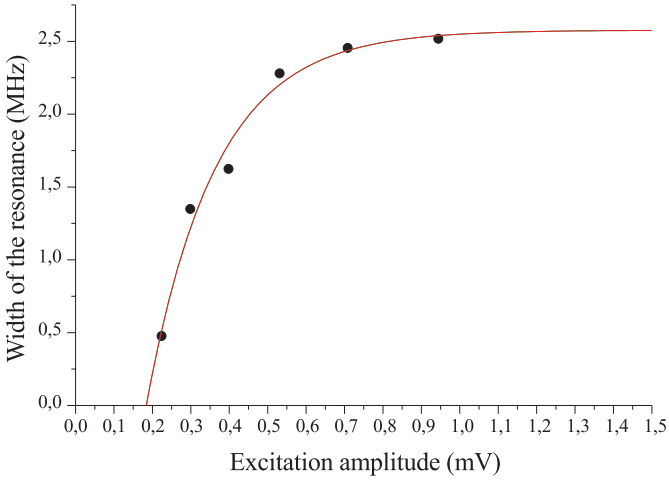

Fig. 9. Threshold behavior of the collective oscillation. The fitted function is $y = y_0 + A(1 - e^{V/V_{thr}})$, which gives a threshold amplitude of $V_{thr} = 0.18 \pm 0.04$ mV.

the damping mechanism. If we assume the same for our case of trapped electrons we expect that the value of the critical voltage amplitude compared to the corresponding value for atomic ions reflects the difference in collisional cross section for ions and electrons. In fact the measured threshold amplitude here is about 0.2 V (Fig. 9) whereas in case of H_2^+ ions in a Paul trap it was of the order of 10 V [18].

5 Conclusion

The appearance of the individual resonance at frequency $2\omega_z$ is the well-known parametric resonance of an harmonic oscillator at quadrupolar excitation. The existence of a minimum amplitude to excite the center-of-mass resonance, however, makes it likely that this is an instability occurring when the trapping parameter a of a Mathieu-type equation for the axial motion under the influence of

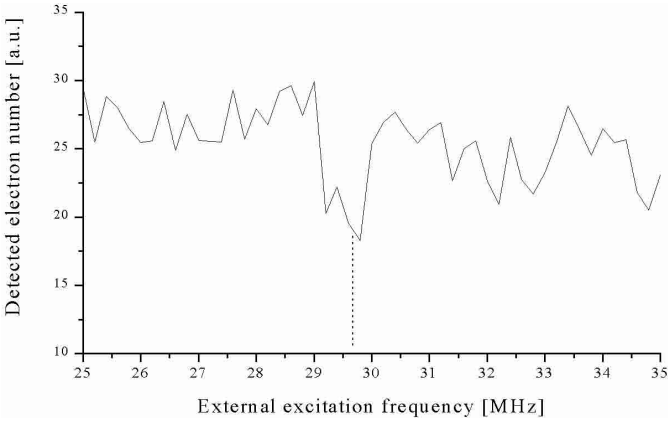

Fig. 10. Motional resonance appearing near $2\nu_z/3$. The dashed line is the calculated frequency from the measured center-of-mass resonance at $2\nu_z$.

an exciting rf-field is the square of an integer n, as discussed above. From equation (15) follows that additional resonances should also occur for $\omega = (2\omega_z/n)$, $n = 2, 3, 4...$ In fact we have observed the same behaviour at $\omega = \omega_z$ $(n = 2)$ where as in the case of the $2\omega_z$ resonance a shifted, broad asymmetric resonance occurs due to the normal dipolar excitation accompanied on the high frequency side by a narrow line which required a threshold amplitude. A search for frequencies at higher values of n in the axial oscillations, as they appear in a Paul trap [22] was difficult because multiples of the magnetron frequency occur in the same frequency range as the expected fractions of $2\omega_z$. At the high amplitudes of the rf-field required for excitation of the fractional resonances the multiples of the magnetron frequency become broad and tend to overshadow the fractional resonances. Some marginal evidence, however, has been obtained in some attempts.

Figure 10 shows an example where a weak resonance of symmetric shape appears at 1/3 of the measured frequency of the $2\omega_z$ center-of-mass resonance. Although no convincing series of motional resonances at fractions of $2\omega_z$ can be reported our occasional observation of weak minima in the stored electron number for different values of $n > 2$ may be considered as support for the interpretation as parametric instabilities.

Our observations may be of some interest in mass spectrometry using Penning traps. Here the mass dependent ion cyclotron frequencies are compared and values for the mass difference or mass ratios are obtained. The cyclotron frequency ω_c can be measured directly by sideband excitation at $\omega = \omega_c' + \omega_m$ or independent measurements of all three fundamental oscillation frequencies ω_c', ω_z, and ω_m using the relation [16]

$$\omega_c^2 = \omega_c'^2 + \omega_z^2 + \omega_m^2. \quad (17)$$

This relation is independent of trap misalignements to first order. When the frequencies are subject to space charge shifts as in the case of large ion clouds, the observed frequencies have to be corrected for these shifts. Using the center-of-mass oscillation this space charge shift would be

eliminated, increasing the precision of mass measurements using large ion clouds. We have checked this by taking the measured frequencies as they appear in Figure 4. The measured sideband at $\omega_c/2\pi$ appears at 122.0 ± 0.8 MHz. From equation (17) we obtain 120.5 ± 0.4 MHz when we take for ω_z the individual axial frequency, while with the center-of-mass resonance we get 121.2 ± 0.3 MHz in much better agreement to the measured sideband.

Our experiment was supported by the Deutsche Forschungsgemeinschaft. We thank S. Ananthamurthy for critically reading the manuscript.

References

1. G. Werth, Hyperf. Interact. **59**, 206 (1995).
2. G. Savard, G. Werth, Annu. Rev. Nucl. Part. Sci. **50**, 119 (2000).
3. D.A. Church, Phys. Rep. **228**, 253 (1993).
4. E. March, J.F.J. Todd, *Practical Aspects of Ion Trap Mass Spectrometry* (CRC, Boca Raton, 1995).
5. Articles in: Phys. Scripta B **59**, Proc. Nobel Symp. on Trapped Charged Particles and Related Fundamental Physics (1995), and: *Trapped Charged Particles and Fundamental Physics*, edited by D. Dubin, D. Schneider, Asilomar (1998), AIP Conf. Procedings **457**.
6. R. Blümel *et al.*, Nature **334**, 309 (1998).
7. T. O'Neill, Hyperf. Interact. **59**, 341 (1995).
8. J.J. Bollinger *et al.*, Phys. Rev. A **48**, 525 (1993).
9. J.J. Bollinger *et al.*, in: *Trapped Charged Particles and Fundamental Physics*, edited by D. Dubin, D. Schneider, AIP Conf. Procedings **457**, 295 (1998).
10. T.M. O'Neill, in: *Non-Neutral Plasma Physics*, edited by C.W. Robertson, C.F. Driscoll, AIP Conf. Proc. **175**, 1 (1988).
11. J.N. Tan, J.J. Bollinger, D.J. Wineland, IEEE Trans. Instr. Meas. **44**, 144 (1995).
12. D.H.E. Dubin, Phys. Rev. Lett. **66**, 2076 (1991).
13. D.J. Heinzen *et al.*, Phys. Rev. Lett. **66**, 2080 (1991).
14. M.D. Tinkle *et al.*, Phys. Rev. Lett. **72**, 352 (1994).
15. C.S. Weimer *et al.*, Phys. Rev. A **49**, 3842 (1994).
16. L.S. Brown, G. Gabrielse, Rev. Mod. Phys. **58**, 233 (1986).
17. D. Wineland, H. Dehmelt, Intern. J. Mass Spectrom. Ion Phys. **16**, 338 (1975).
18. R. Alheit *et al.*, Phys. Rev. A **56**, 4023 (1997).
19. P.K. Ghosh, *Ion Traps* (Clarendon Press, Oxford, 1995).
20. J. Yu, M. Desaintfuscien, F. Plumelle, Appl. Phys. B **48**, 51 (1989).
21. R.S. van Dyck, F.L. Moore, D.L. Farnham, P.B. Schwinberg, Phys. Rev. A **40**, 6308 (1989).
22. M.A.N. Razvi *et al.*, Phys. Rev. A **58**, R34 (1998).
23. L.D. Landau, E.M. Lifschitz, *Mechanics* (Pergamon, Oxford, 1960).